Tang *et al. BMC Genomics* (2025) 26:403
https://doi.org/10.1186/s12864-025-11535-8

BMC Genomics

RESEARCH Open Access

Genome-wide characterization and expression analysis of *WRKY* family genes in the biosynthesis of triptolide in *Tripterygium wilfordii*

Limei Tang[1], Xinyu Qi[1], Jiayu Chen[1], Yujun Zhao[2], Junhao Gu[3], Shanshan Zhu[3*], Wei Gao[4*] and Lichan Tu[1*]

Abstract

Background WRKY transcription factors play a vital role in regulating plant growth, development, and secondary metabolism. *Tripterygium wilfordii* is a medicinal plant that has been widely utilized in rheumatoid arthritis therapy; it contains triptolide, a prominent bioactive constituent exhibiting potent anti-inflammatory and anti-tumor properties. However, the mechanism underlying the regulatory effects of WRKY on triptolide biosynthesis is poorly understood.

Results In this study, 95 *TwWRKY* genes were identified in the *T. wilfordii* genome, which were divided into three groups. Phylogenetic analysis indicated that the TwWRKY were conservative relative to other plants. Collinearity analysis revealed that gene duplications played a crucial role in the evolution of this gene family. Transcriptome data from various plant tissues were integrated by correlation analysis, and a gene-to-metabolite network was successfully mapped; consequently, 32 *TwWRKY* genes were selected as potential regulators of triptolide biosynthesis. Furthermore, the expression changes in the 32 *TwWRKY* genes were analyzed following methyl jasmonate (MeJA) induction, and the key candidates likely to regulate the biosynthesis of triptolide were screened. Finally, we performed subcellular localization on the key candidate gene *TW23G00056.1* and found that it plays its biological role in the nucleus.

Conclusion Our study provides a valuable resource for further research on TwWRKY in *T. wilfordii*. The candidate genes reported here lay the foundation for elucidating the regulatory mechanism of triptolide.

Keywords WRKY, *Tripterygium wilfordii*, Triptolide, Gene expression

*Correspondence:
Shanshan Zhu
zhushanshan1@nbu.edu.cn
Wei Gao
weigao@ccmu.edu.cn
Lichan Tu
tulichan@hzcu.edu.cn
[1]Department of Pharmacy, School of Medicine, Hangzhou City University, Hangzhou, Zhejiang 310015, China
[2]State Key Laboratory for Quality Ensurance and Sustainable Use of Dao-di Herbs, National Resource Center for Chinese Materia Medica, China Academy of Chinese Medical Sciences, Beijing 100700, China
[3]School of Marine Sciences, Ningbo University, Ningbo, Zhejiang 315211, China
[4]School of Traditional Chinese Medicine, Capital Medical University, Beijing 100069, China

Introduction

Tripterygium wilfordii, a significant member of the Celastraceae family within the genus Tripterygium, is widely distributed across Eastern and Southern China, Korea, and Japan [1]. This vine shrub, commonly known as Lei Gong Teng, is a traditional medicine utilized in treating rheumatism and skin disease and as a botanical insecticide [2]. In Chinese mythology, Leigong is a God of thunder, reflecting the potency of this plant, which was first recorded in the "Shennong Ben Cao Jing" during the Han Dynasty. In addition, *T. wilfordii* contains multiple secondary metabolites, with triptolide showing significant potential for pharmaceutical development [3].

Triptolide was discovered in 1972 as the first diterpenoid triepoxide extracted from *T. wilfordii*'s ethanol extracts [4]. Owing to its unique molecular structure and multiple therapeutic activities, extensive research has been conducted to explore its therapeutic applications [5]. Triptolide is the most powerful and broadly active anti-inflammatory/immunomodulating natural product ever discovered [6, 7] with a 100–200 times higher potency compared to crude plant extracts [8]. In recent years, researchers from all over the world have investigated its anti-tumor, anti-fertility, antiproliferative, and anti-cystogenesis effects [7, 9–11]. A large number of studies have analyzed the therapeutic effects of triptolide and its derivatives on various diseases, including rheumatoid arthritis, psoriatic arthritis, systemic lupus erythematosus, nephritis, asthma, Behcet's disease, organ transplantation, and numerous forms of tumors [7, 12–17]. However, triptolide is extracted at a meager rate of 6–16 ng/g [18], which underscores the necessity for advancing our understanding of its biosynthetic pathway and regulatory mechanisms to enhance its production both in native plants and through heterologous systems.

The WRKY is one of the largest families of transcription factors in the plant kingdom [19]. It plays a vital role in regulating various biological processes, not only in response to biotic and abiotic stresses but also in secondary metabolism regulation. For instance, AtWRKY18 and AtWRKY40 negatively regulate the expression of defensive positive genes and increase the biosynthesis of camalexin [20]. Another study revealed that overexpression of *OsWRKY62* and *OsWRKY76* enhanced plant defense against rice blast and bacterial leaf blight disease [21]. In recent years, researchers have also explored the regulatory effects of WRKY transcription factors on secondary metabolisms, such as terpenoids; overexpression of *SmWRKY1* significantly upregulated the transcription of pathway genes and production of tanshinone [22]. In addition, CrWRKY1 positively regulated several key terpenoid indole alkaloid pathway genes [23]. A previous study reported that the biosynthesis of maize terpenoid phytoalexins was regulated by ZmWRKY79 by binding W-box or WLE *cis*-elements in the promoters of *An2* and *ZmTPS6* [24].

Despite these advances, the transcriptional regulation of the triptolide biosynthetic pathway remains incompletely understood, especially the role of WRKY transcription factors. Our study aims to bridge this gap by identifying and characterizing a total of 95 *TwWRKY* genes in the *T. wilfordii* genome, analyzing their sequence features, motifs, and bioinformatic characteristics. Considering the established role of methyl jasmonate (MeJA) in stimulating secondary metabolism and its effect on most of the *WRKY* genes [25], transcriptomic data from MeJA-induced samples were analyzed. These analyses provide further insights into the MeJA-induced changes in the expression patterns of *TwWRKY* genes in suspension cells. Moreover, transcriptomic data from tissue expression profiles were analyzed to determine the TwWRKY-mediated regulatory networks involved in triptolide biosynthesis. This study deepens our understanding of the role of WRKY in response to MeJA and provides key regulators of triptolide biosynthesis.

Results

Identification of *WRKY* genes in the *T. wilfordii* genome

The ITAK program identified a total of 95 *TwWRKY* genes in the genome of *T. wilfordii* based on the WRKY domain (PF03106) [26]. Except for chromosome 5, a total of 95 *WRKY* genes were distributed on the other 22 chromosomes (Fig. 1). The *TwWRKY* genes are mostly distributed on chromosomes 4, 10, 13, 18, and 21, of which chromosome 18 was the most distributed, with a total of 11 *TwWRKYs*. The 95 identified TwWRKY proteins had a length ranging between 124 and 1059 amino acids, with a molecular weight (mw) of 14.3 to 115.6 kDa. The isoelectric point (pI) of these TwWRKYs ranged from 5.02 to 10.16, indicating that they were widely distributed in different microcellular environments (Table S1). Sequence analysis of 95 WRKY proteins revealed that most WRKY proteins had a conserved "WRKYGQK" motif, whereas only a TwWRKY (TW04G00295.1) had a "WRKYGKK" motif (Table S1). These results were consistent with previous studies reporting that the Q site in WRKYGQK was preferentially mutated into K [27]. Therefore, WRKYs are more conservative than other species, such as *Salvia miltiorrhiza* [28] and soybean [27].

Phylogenetic analysis of the *T. wilfordii* WRKY family

To investigate the evolution and topological structure of the WRKY protein family in *T. wilfordii*, an ML phylogenetic tree was constructed using the JTTDCMut model based on the 95 TwWRKY proteins and 72 AtWRKY proteins (Fig. 2). All 95 TwWRKYs were unevenly clustered into three groups [19]. Among them, 23 TwWRKY proteins were categorized into Group I. The other 56

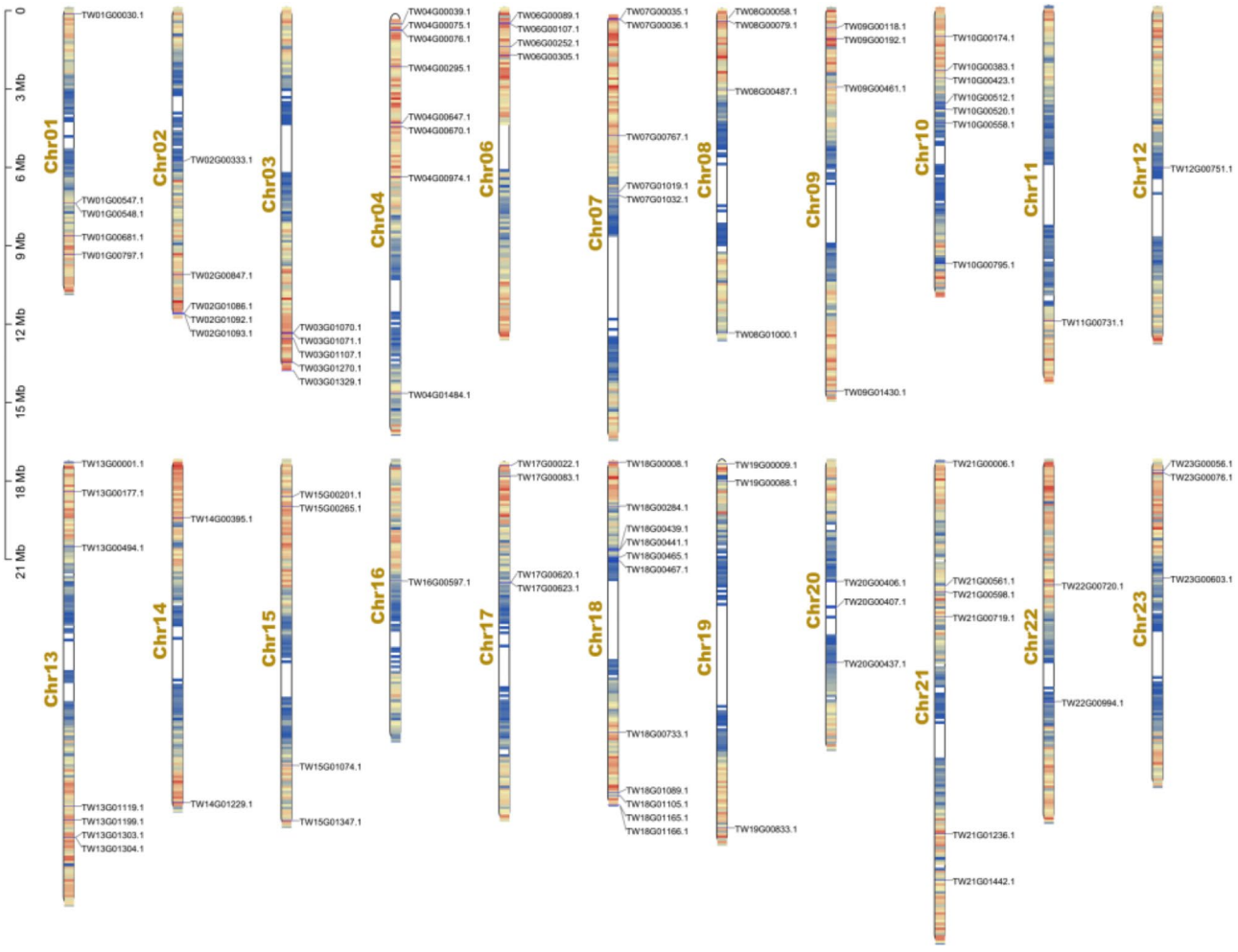

Fig. 1 The chromosomal location of *TwWRKYs* in *T. wilfordii*. The chromosome number is shown on the left side of each chromosome, and the ID of each *TwWRKY* is displayed on the right side of the chromosome. The color on the chromosome represents the gene density, with red representing high gene density

TwWRKY proteins were assigned to Group II, which contained only one WRKY domain and accounted for 58.9% of the total TwWRKYs. The 56 TwWRKY proteins of Group II were further divided into five specialized subgroups (Group II a-e). Specifically, 4 TwWRKY proteins were clustered into Group II-a, 13 TwWRKY proteins were clustered into Group II-b, 20 TwWRKY proteins were clustered into Group II-c, 6 TwWRKY proteins were clustered into Group II-d, and 13 TwWRKY proteins were clustered into Group II-e. The remaining 16 TwWRKYs were categorized under Group III. This detailed analysis not only elucidates the evolutionary relationships among these TwWRKYs but also sheds light on their potential functional diversification within *T. wilfordii*.

Motif composition analysis of TwWRKY proteins

To further study the diversity and similarity of functional regions among *WRKY* genes in *T. wilfordii*, 20 motifs in TwWRKY protein sequences were predicted by the MEME online software (Fig. 3). The 20 motifs were composed of 15 to 50 amino acids and most appeared in special groups. Only two motifs (motif 1 and motif 2) were common to all groups. Motif 1 was found to encode the heptapeptide stretch WRKY domain, while motif 2 encoded the conserved zinc finger structure. Motif 17 and motif 19 were unique to group II-e, motif 8 was unique to group II-b, motif 5 and motif 7 only appeared in groups II-a and II-b, motif 9 only appeared in groups II-d and II-e, and motif 13 only appeared in groups II-d and III. Concurrently, the groups with the same motifs were all adjacent in the phylogenetic tree.

Collinearity analysis of *WRKY* genes

Expansion of gene families may drive the evolution of gene families [29, 30]. Therefore, duplication event analysis of the *TwWRKY* genes was performed using MCScanX, revealing a total of 98 segmental-duplicated gene

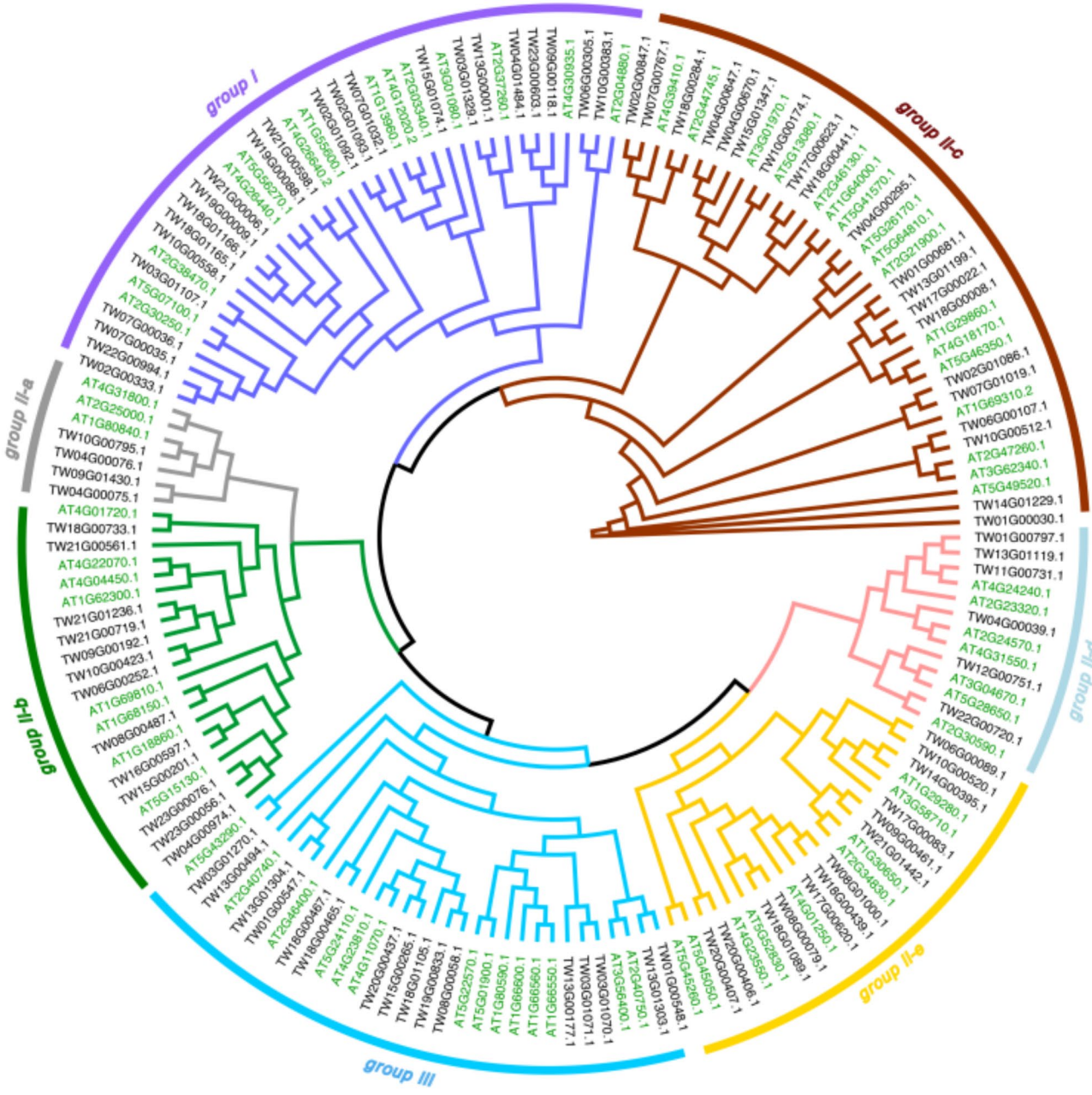

Fig. 2 Maximum likelihood (ML) tree of the WRKY proteins from *T. wilfordii* (black) and *Arabidopsis thaliana* (green). The tree was constructed from amino sequences using phylosuite software using the IQ-TREE program. Different colored branches represent different groups/subgroups

pairs on the *T. wilfordii* chromosomes, as shown in Fig. 4. In addition, gene tandem duplication was detected in the *TwWRKY* genes to investigate other potential gene amplification mechanisms in the *WRKY* family. Finally, five gene pairs showing gene tandem duplications were detected in the *WRKY* gene family, including TW03G01070.1/TW03G01071.1, TW04G00075.1/TW04G00076.1, TW13G01303.1/TW13G01304.1, TW18G00466.1/TW18G00467.1, and TW20G00406.1/TW20G00407.1.

To further explore the evolution of *TwWRKY* genes, collinearity analysis was performed on the *WRKY* genes of *T. wilfordii* and five other plants, including monocotyledonous and dicotyledonous species closely and distantly related to *T. wilfordii.* Collinearity analysis identified 207 pairs of homologous *WRKY* genes on the chromosomes of *T. wilfordii* and *Populus trichocarpa*, including 82 *TwWRKYs*. Specifically, 113 pairs of homologous *WRKY* genes were found on the chromosomes of *T. wilfordii* and *A. thaliana*, including 75 *TwWRKYs*; a total of 115 pairs of homologous *WRKY* genes were

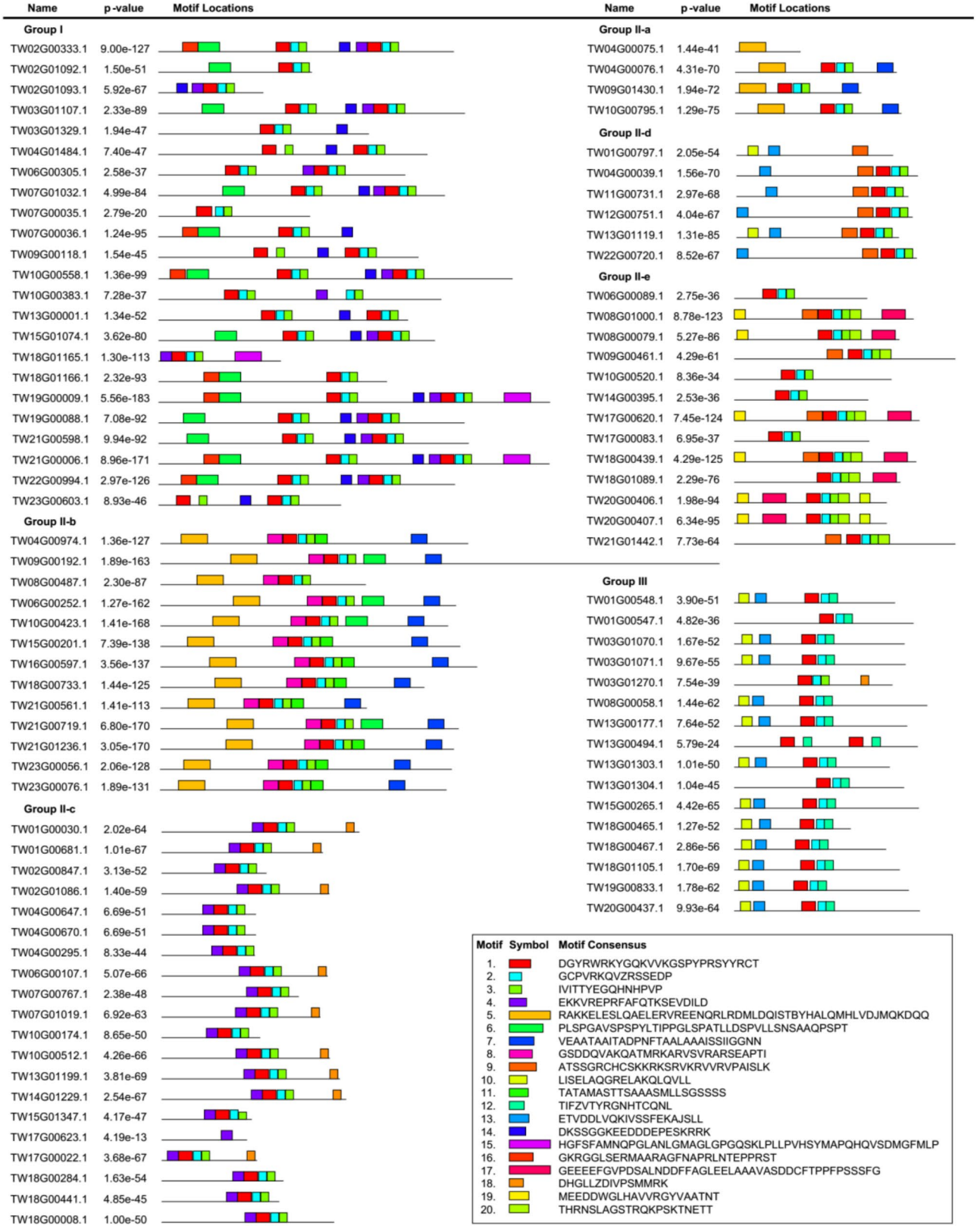

Fig. 3 Schematic diagram of 20 motifs in TwWRKY proteins. The 20 colored boxes represent 20 motifs. The size of the box indicates the length of the motif

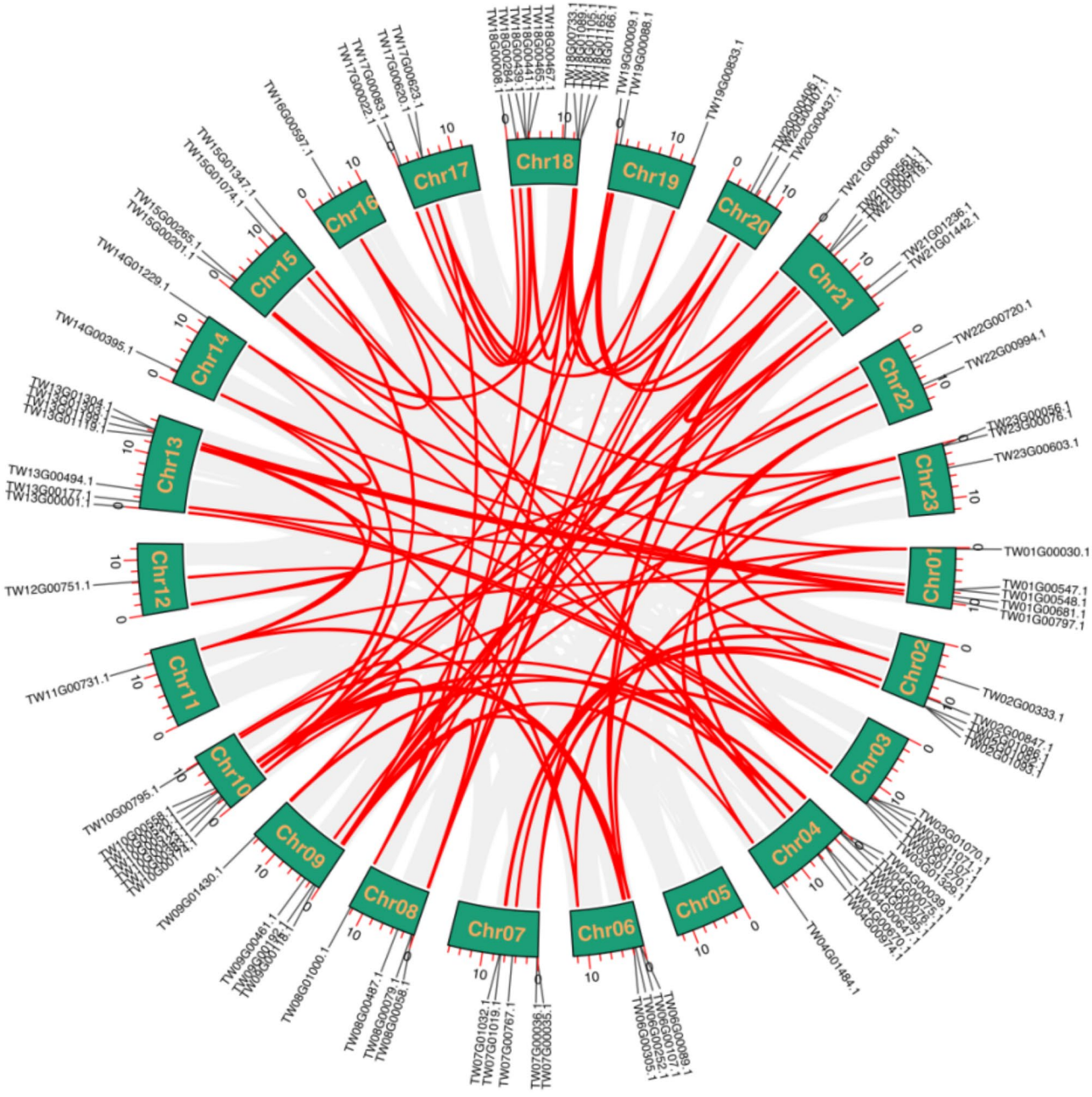

Fig. 4 Segmental duplication events and inter-chromosomal relationships between *TwWRKY* genes. The gray lines indicate all collinear blocks in the *T. wilfordii* genome. The red lines indicate *TwWRKY* segmental duplication genes

detected on the chromosomes of *T. wilfordii* and *Salvia miltiorrhiza*, including 72 *TwWRKYs*. Furthermore, 123 pairs of homologous *WRKY* genes were found on the chromosomes of *T. wilfordii* and *Vitis vinifera*, including 76 *TwWRKYs*; a total of 20 pairs of homologous *WRKY* genes were located on the chromosomes of *T. wilfordii* and *Zea mays*, including 11 *TwWRKYs* (Fig. 5). These findings suggest that WGD and segmental duplication play an essential role in the evolution of the *TwWRKY* gene family.

Expression analysis of *TwWRKY* genes in tissues

The presence of active ingredients in plants, such as triptolide [31], celastrol [32], and tanshinone [33], is usually tissue-specific. Growing evidence indicates that genes related to the biosynthesis of active components also show tissue-specific expression patterns [31, 34, 35]. To explore the potential role of TwWRKYs in triptolide biosynthesis, the expression of 95 *TwWRKY* genes was detected in various tissues (leaf, root bark, root phloem, root xylem, stem bark, peeled stem, and flower) from

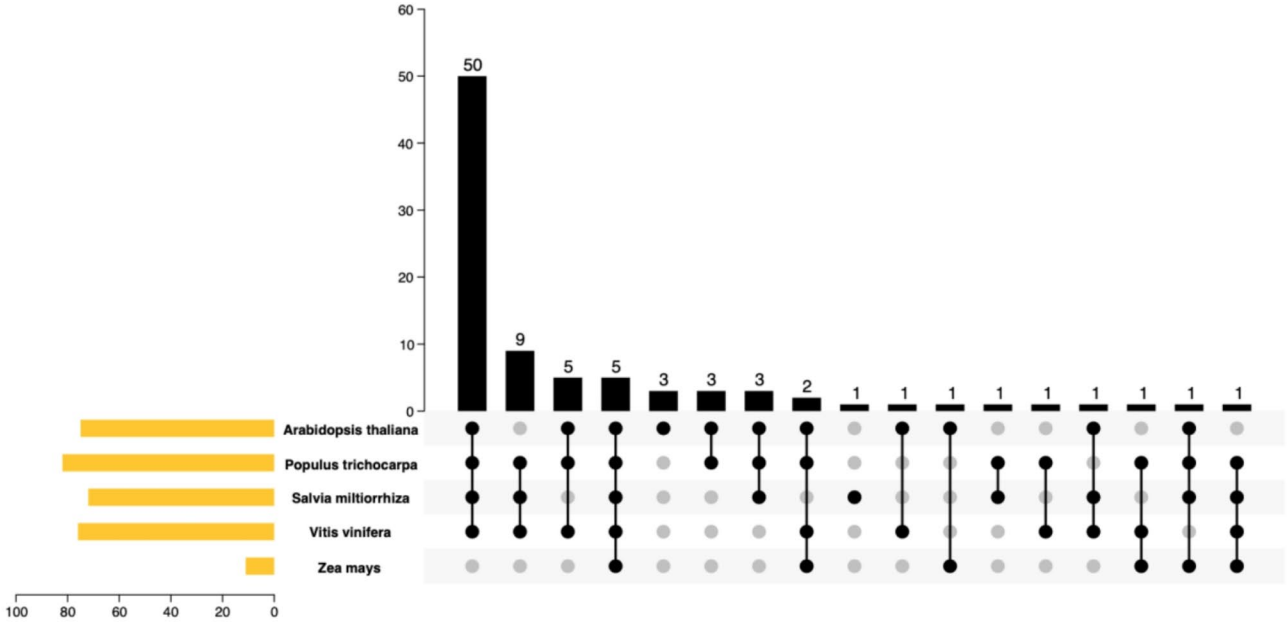

Fig. 5 Collinearity analysis of *WRKY* genes in the chromosomes of *T. wilfordii* and five other representative species

transcriptome data [31]. 95 *TwWRKY* genes were specifically expressed in different plant tissues (Fig. 6), highlighting their diverse functions in *T. wilfordii*. All *TwWRKY* genes were divided into several clusters, with 20 *TwWRKY* genes being most highly expressed in root bark, which was consistent with the content of triptolide in *T. wilfordii* [31]. Additionally, high expression of *TwWRKY* was primarily found in stem bark and peeled stems (Table S2), which suggested that the *WRKY* gene plays a more important role in these two tissues.

Integration of metabolites accumulation and gene expression analysis

To gain further insight into the regulation of *TwWRKY* genes in triptolide biosynthesis, a correlation network analysis was conducted to create a co-regulation pattern of metabolite-to-gene for various tissues. 32 compounds enriched in roots were selected as yet-unknown intermediates or side compounds of the triptolide pathway, as detailed in our previous studies [31]. Subsequently, the Pearson correlation coefficient was calculated between metabolites and genes with a correlation coefficient > 0.7 as the cutoff value in tissues (Fig. 7).

A total of 32 *TwWRKY* genes in the regulation network of tissues were strongly correlated with compounds related to triptolide biosynthesis (Fig. 7). Interestingly, of the 32 *TwWRKY* genes found in the tissue network regulation, 8 *TwWRKY* genes belonged to Group II-c, 6 *TwWRKY* genes belonged to Group I, 6 *TwWRKY* genes belonged to Group II-b, 4 *TwWRKY* genes belonged to Group II-d, 3 *TwWRKY* genes belonged to Group II-e, 3 *TwWRKY* genes belonged to Group III, and 2 *TwWRKY* genes belonged to Group II-a. These results indicate that *TwWRKY* genes in Group II-c were most closely associated with triptolide biosynthesis and were likely the key regulatory group of triptolide biosynthesis.

Furthermore, the tissues regulation networks revealed that two *TwWRKY* genes (*TW06G00089.1*, *TW23G00056.1*) were strongly correlated with almost all compounds, including triptolide and triptophenolide. The correlation coefficients between *TW06G00089.1* with triptolide and triptophenolide in the tissue regulation network were 0.767 and 0.792, respectively. The correlation coefficients between *TW23G00056.1* with triptolide and triptophenolide were 0.811, and 0.821, which may regulate and promote triptolide biosynthesis.

Expression analysis of *TwWRKY* genes in response to MeJA

Previous studies reported that MeJA could induce terpenoids and *WRKY* genes [36–39]. To gain a deeper understanding of the role of *WRKY* genes in the biosynthesis of triptolide, the expression of *TwWRKY* genes was analyzed after induction by MeJA. After 48 h of MeJA induction, a significant increase was observed in cellular levels of triptolide and its biosynthetic intermediate, triptophenolide [31]. Additionally, most genes involved in the triptolide biosynthetic pathway showed significant changes within 48 h [31]. Therefore, the expression of the *WRKY* gene, which regulates the triptolide pathway genes, should respond to MeJA treatment earlier than 48 h. To test this hypothesis, we analyzed transcriptome data at 0 h, 4 h, 12 h, 24 h, and 48 h post-MeJA induction in suspension cells. This analysis was aimed to investigate the transcriptional changes of 32 *TwWRKY* genes and to identify

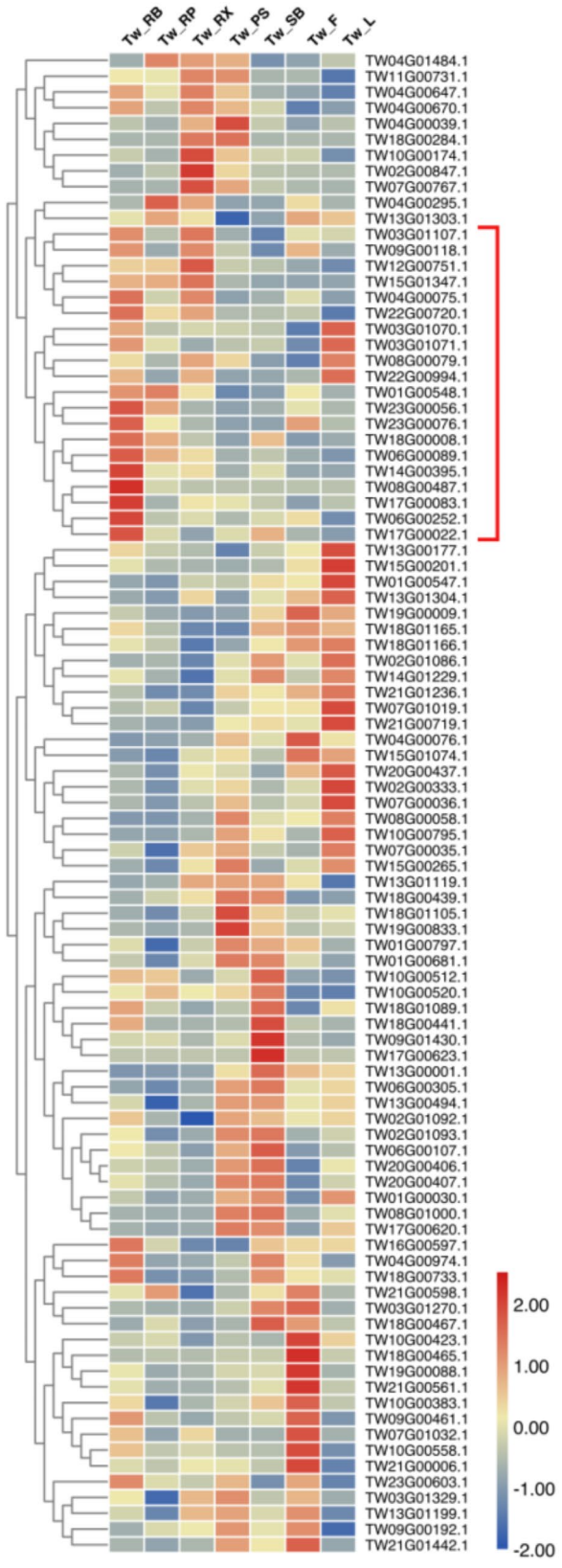

Fig. 6 The expression profile of *TwWRKY* genes in seven tissues

potential candidate TwWRKYs that respond to MeJA and may regulate the triptolide biosynthetic pathway genes (Fig. 8). Compared with the control group, the results showed that 11 of 32 *TwWRKY* genes were up-regulated after MeJA induction. Among them, *TW03G01107.1*, *TW04G00647.1*, *TW13G00001.1*, *TW17G00083.1*, and *TW23G00056.1*, were the most probable candidates for positively regulating triptolide biosynthesis. In contrast, 13 *TwWRKY* genes were down-regulated, including *TW02G00847.1*, *TW06G00252.1*, *TW07G00767.1*, and *TW12G00751.1*, which were candidates for negatively regulating triptolide biosynthesis.

Subcellular localization analysis of TwWRKY

To date, the subcellular localization of TwWRKY proteins remains unclear. Based on comprehensive gene expression profiles and correlation network analysis, TW23G00056.1 was identified as a candidate for subcellular localization studies. To explore its biological activity, the full-length protein sequence of TW23G00056.1 fused to the N-terminus of the GFP was transformed into Arabidopsis protoplasts. The pAN580-GFP vector was used as the control and the fluorescence of the control GFP was distributed throughout the cell. NLS-mkate acted as the nuclear localization marker to observe whether TW23G00056.1 localizes within the nucleus. Finally, the fluorescence of pAN580-TW23G00056.1-GFP is specifically observed in the nucleus (Fig. 9). This finding indicates that TW23G00056.1 is localized to the nucleus.

Discussion

T. wilfordii has attracted significant interest due to its remarkable pharmacological potential and diverse secondary metabolites. Notably, triptolide, a potent diterpenoid extracted from this plant, exhibits remarkable efficacy against a broad spectrum of cancer types, especially pancreatic cancer cells [15, 40]. Despite its promising therapeutic properties, the scarcity of triptolide in both its natural plant form and suspension cell cultures presents a significant challenge, limiting further pharmaceutical exploration and application due to supply constraints. Consequently, various techniques have been applied to increase the production of triptolide, including metabolic engineering and chemical synthesis. This study combined genomic and transcriptomic data of *T. wilfordii*, focusing on the regulatory mechanisms of WRKY transcription factors on triptolide biosynthesis. This study aims to identify new avenues for enhancing the production of this valuable compound.

Although WRKY plays a vital role in the biosynthesis of secondary metabolism, the regulation of triptolide biosynthesis by WRKY remains largely unknown. Therefore, a comprehensive analysis was conducted to investigate the WRKY family in *T. wilfordii*. This study identified

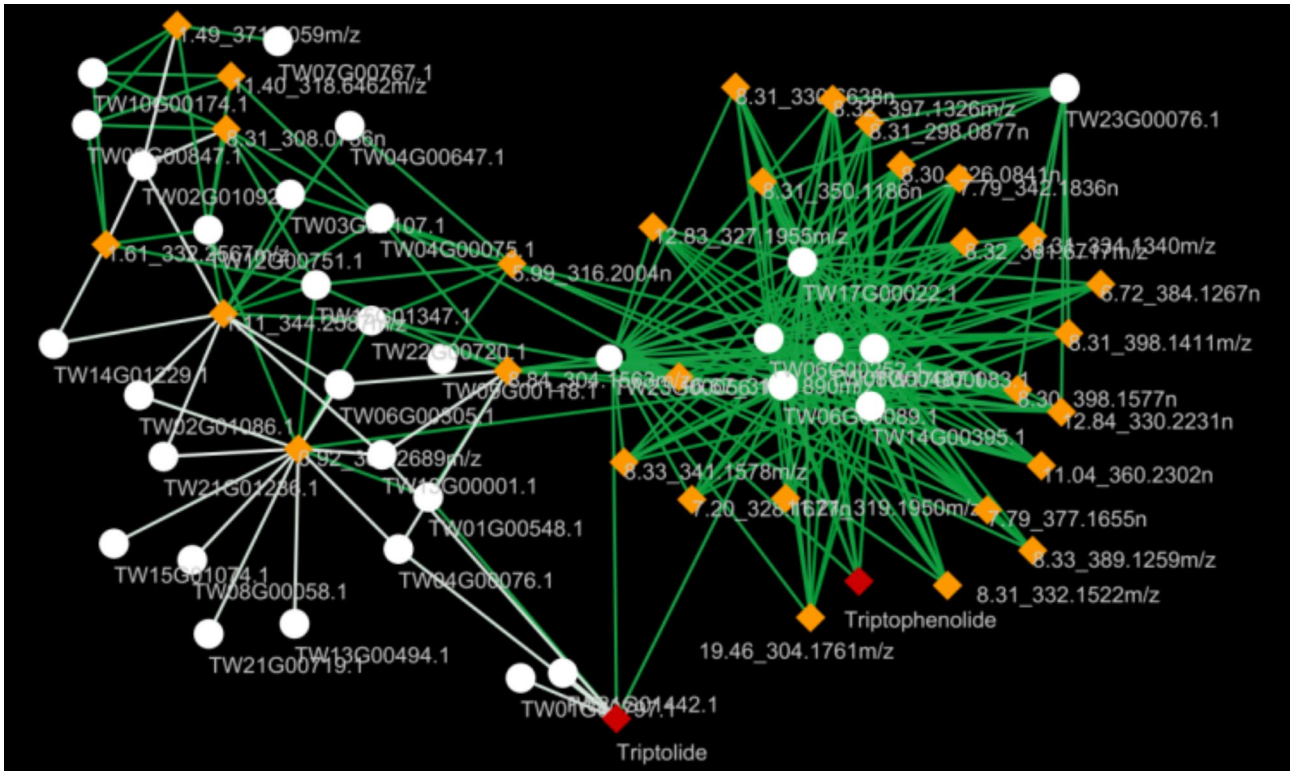

Fig. 7 The regulation networks of *TwWRKY* genes in triptolide biosynthesis. *TwWRKY* genes are represented by circles, and metabolites related to triptolide biosynthesis are represented by diamonds. Edges represent a linear correlation coefficient > 0.7. Green lines indicate a positive correlation, while white lines indicate a negative correlation

95 *TwWRKY* genes through genomic data, which were unevenly dispersed across 22 chromosomes, except chromosome 5. The protein sequence analysis showed that the WRKY proteins in *T. wilfordii* were relatively conservative, and only one "WRKYGQK" motif of TwWRKY was mutated to "WRKYGKK", which may affect the binding of *cis*-elements and regulatory function [41]. Subsequently, these 95 TwWRKY proteins were classified into three distinct groups based on the ML phylogenetic tree. Notably, group II emerged as the predominant cluster, harboring 5 subfamilies and accounting for 58.9% of all classified genes. These findings were similar to other species, such as 58% in *A. thaliana* [19]. The phylogenetic framework not only reveals evolutionary relationships but also facilitates the targeted identification of genes implicated in specific biological processes. AtWRKY18 and AtWRKY40 have been demonstrated to regulate the expression of *DXS*, *DXR*, *GGPPS*, and *CPS* genes in the MEP-dependent pathway [42]. Diterpenoids are primarily synthesized through the MEP pathway [43]. Triptolide, the most significant diterpenoid compound found in *T. wilfordii*, has been reported to have its content influenced by the expression levels of *TwDXS* [44], *TwDXR* [45], *TwGGPPS* [46], and *TwCPS1/4* [47]. Phylogenetic tree construction has been a common method for studying gene evolution and gene function prediction, and neighboring genes often have similar functions [48–50]. Consequently, four TwWRKYs (TW04G00075.1, TW04G00076.1, TW09G01430.1, and TW10G00795.1), which belong to group II-a and were closely related to AtWRKY18 and AtWRKY40, may play a role in the biosynthesis of diterpenoids similar to AtWRKY18 and AtWRKY40. However, as shown in Fig. 7, only two of these four genes, *TW04G00075.1* and *TW04G00076.1*, exhibited strong correlations ($r > 0.7$) with compounds associated with triptolide biosynthesis. Notably, the white line representing *TW04G00076.1* and triptolide indicates a significant negative correlation (Fig. 7). Additionally, the expression of *TW04G00076.1* was significantly down-regulated after MeJA induction (Fig. 8), which contrasts with the accumulation pattern of triptolide. These findings lead us to speculate that TW04G00076.1 may play a crucial role as a negative regulator of triptolide biosynthesis.

The primary aim of this study was to identify potential *TwWRKY* genes involved in the biosynthesis of triptolide. Gene expression levels for 95 *TwWRKYs* were obtained by analyzing available transcriptome datasets. Significant differences in the expression of some *TwWRKY* transcription factors were observed in tissues and suspension cells. Almost all *TwWRKY* genes were expressed in tissues, but some *TwWRKYs* were notably silent in suspension cells.

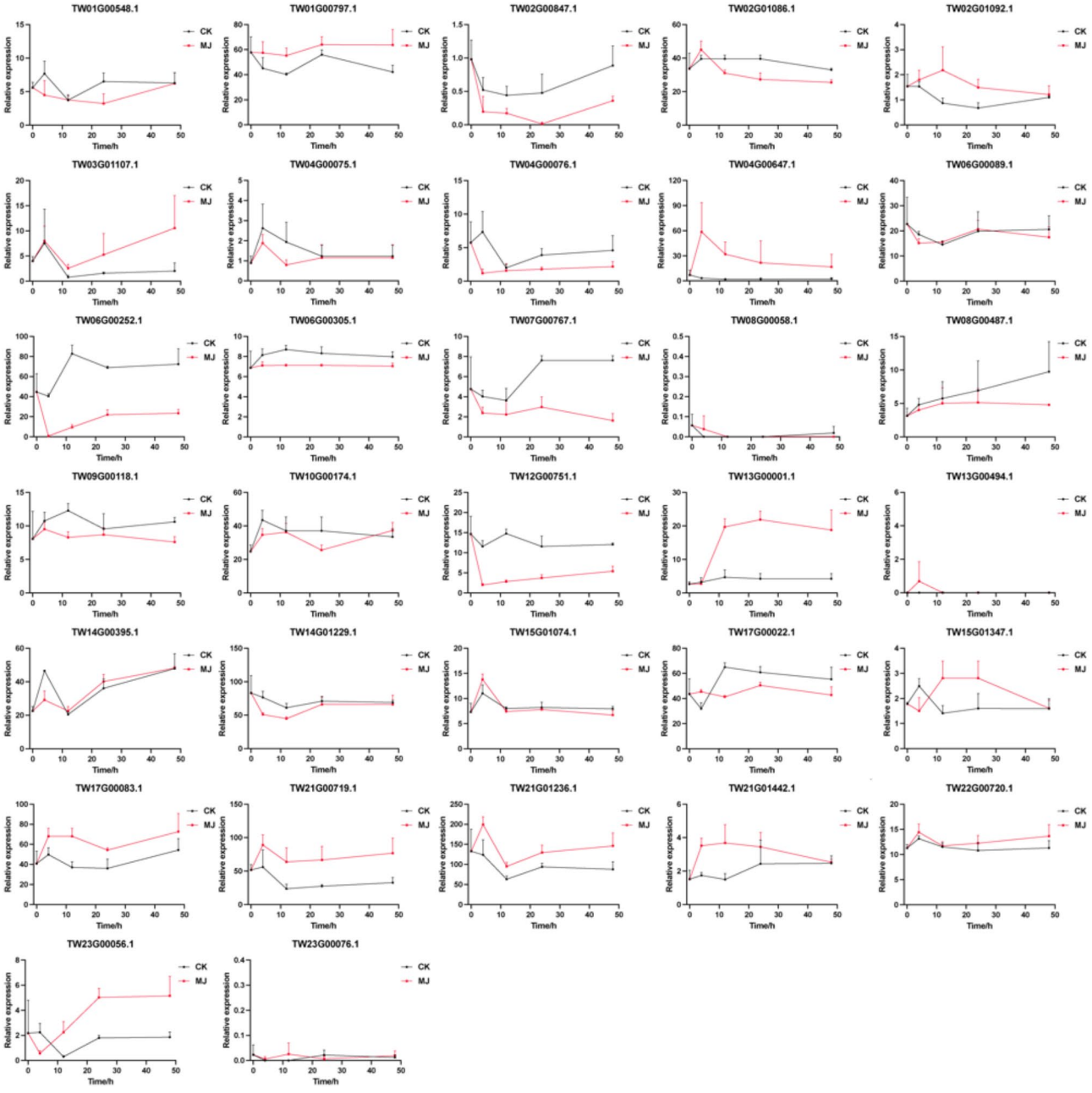

Fig. 8 Expression patterns of *TwWRKY* response to MeJA. CK indicates the control group, and MJ denotes the group of MeJA treatment. Transcriptome data were collected from the CK and MJ groups at five time points (0, 4, 12, 24, and 48 h) of suspension cells to determine the expression [31]. Error bars, mean + SD ($n = 3$ biologically independent samples)

These *WRKY* genes may be related to the existing state of plants, such as TW08G00058.1, which was highly expressed in leaves and peeled stems but not in suspension cells under all conditions, suggesting its potential involvement in tissue-specific functions. Moreover, tissue transcriptomes were explored to construct gene-to-metabolite correlation networks, uncovering a subset of *TwWRKY* genes that were strongly associated with diterpenoids involved in the triptolide biosynthesis. Notably, group II-c members emerged as the closest associates of triptolide biosynthesis within the tissue network. As shown in Figs. 7, 32 TwWRKYs were found to potentially regulate triptolide biosynthesis, with particular emphasis on TW06G00089.1 and TW23G00056.1. These two genes displayed robust correlations with almost all compounds, including triptolide and triptophenolide, in the tissue regulatory network. Importantly, TW23G00056.1 was significantly upregulated following MeJA induction. Subcellular localization experiments have demonstrated that TW23G00056.1 is localized within the nucleus. This

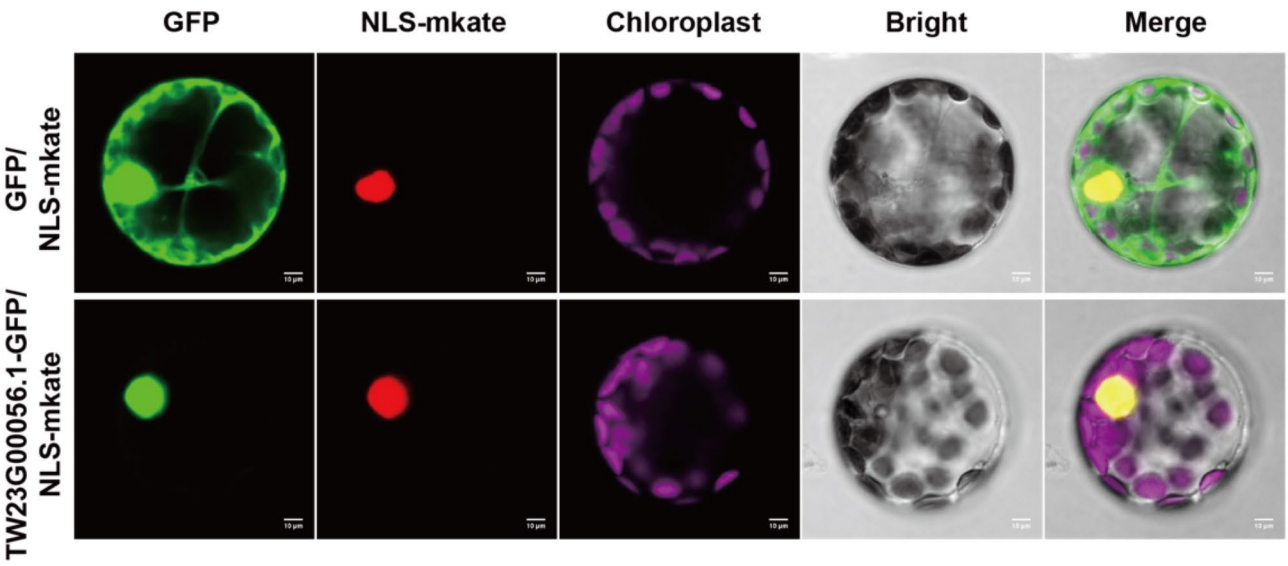

Fig. 9 Subcellular localization of the TW23G00056.1 protein. Green fluorescence represents the GFP signal and red fluorescence indicates nuclear localization marker (NLS-mkate). Scale bars = 10 μm

finding suggests that, like most WRKY genes involved in regulating gene expression [51–54], TW23G00056.1 likely performs its transcriptional regulatory function within the nuclear environment. Given that the genes involved in the triptolide biosynthetic pathway are distributed on different chromosomes in the nucleus [31, 55], the result of subcellular localization further supports our hypothesis that TW23G00056.1 may act as a key factor in regulating the biosynthetic pathway genes of triptolide in the nucleus.

In summary, while deciphering the regulatory mechanism of biosynthetic pathways of triptolide remains a formidable challenge, this study identified candidate TwWRKYs, contributing to future investigations into the roles of TwWRKYs in triptolide biosynthesis. Our findings facilitate the genetic improvement of *T. wilfordii* to increase the yield of triptolide in the future.

Materials and methods

Identification of *TwWRKY* genes

The *T. wilfordii* genome was downloaded from the National Center for Biotechnology Information (NCBI) database (accession number: JAAARO000000000). TwWRKYs were annotated using the ITAK program (http://itak.feilab.net/cgi-bin/itak/index.cgi) [26], which identified *WRKY* genes based on required domain (PF03106). Finally, 95 *WRKY* genes were identified in the *T. wilfordii* genome. The molecular weight (mw) and theoretical isoelectric point (pI) of TwWRKYs were predicted using the ProtParam tool on the ExPASy server (https://web.expasy.org/protparam/).

Multiple sequence alignment, maximum likelihood tree, and motif analysis

The protein sequences of 72 AtWRKYs were downloaded from the Arabidopsis Information Resources (TAIR: http://www.Arabidopsis.org/). The multiple sequence alignment of all *WRKY* genes in *T. wilfordii* and *Arabidopsis thaliana* was performed using the MAFFT program in phylosuite software. Subsequently, the phylogenetic tree was constructed using the maximum likelihood method (bootstrap test was replicated 10000 times) using the IQ-TREE program in phylosuite software.

MEME online software (http://meme-suite.org/tools/meme) was employed to predict the conserved motifs for all *TwWRKY* genes. The following parameters were set: 20 motifs with Any Number of Repetitions (anr), and an optimal motif width of 8 to 50 residues.

Gene localization, gene duplication, and collinearity analysis

Chromosomal localization of the *TwWRKY* genes was performed using *T. wilfordii* genome data and visualized by the TBtools software [56]. Subsequently, MCScanX software was utilized for gene duplication analysis to explore the evolutionary mechanisms of *TwWRKY* genes. The results were visualized using Circos software in TBtools [56]. Among the other species with published genomes, *Populus trichocarpa* was selected due to its close relation to *T. wilfordii*. Moreover, the more distantly related Salvia miltiorrhiza, *Arabidopsis thaliana*, *Vitis vinifera*, and *Zea mays* were selected for collinearity analysis using MCScanX in TBtools [56].

Expression analysis of MeJA-induced suspension cells and various tissues

Previous studies have reported that MeJA can upregulate terpenoid biosynthesis and WRKY gene expression [36–39]. Given that triptolide exhibits tissue-specific distribution patterns [31], we selected tissue-specific transcriptomes and MeJA-induced cell transcriptomes to further analyze the expression profiles of WRKY genes, aiming to identify key WRKY regulators involved in the biosynthesis of triptolide. Transcriptome data of MeJA-induced suspension cells and different tissues were previously uploaded to the SRA database (https://www.ncbi.nlm.nih.gov/sra), including SRX7094753, SRX7094754, SRX7094755, SRX7094756, SRX7094757, SRX7094758, SRX7094759, SRX7094760, SRX7094761, SRX7094763, SRX7094764, SRX7094765, SRX7094766, SRX7094767, SRX7094768, SRX7094782, SRX7094783, SRX7094784, SRX7094785, SRX7094786, SRX7094788, SRX7094790, SRX7094791, SRX7094792, SRX7094793, SRX7094794, SRX7094795, SRX7094739, SRX7094740, SRX7094751, SRX7094762, SRX7094776, SRX7094787, SRX7094798, SRX7094771, SRX7094772, SRX7094749, SRX7094750, SRX7094752, SRX7094773, SRX7094741, SRX7094742, SRX7094743, SRX7094744, SRX7094745, SRX7094746, SRX7094747, and SRX7094748 [31]. The expression profiles of *TwWRKY* genes were mapped with *TwWRKY* gene nucleotide sequence using TopHat2 [57]. Furthermore, the expression level (RPKM value) for each *TwWRKY* gene was calculated by HTSeq [58] using default parameters. Then, DESeq2 [59] was used to normalize gene expression (BaseMean) in each sample, and an adjusted p-value < 0.05 was used to identify differentially expressed genes (DEGs) between groups.

Correlation network analysis for triptolide and TwWRKY genes

Gene-to-metabolite regulatory networks were constructed by integrating datasets of metabolite accumulation and gene expression, following previously reported methodologies [60]. The metabolite data were obtained using the UPLC/Q-TOF MS from previous study [31] and are available from the corresponding author on reasonable request. We selected 32 metabolite peaks that exhibited significant changes by MeJA treatment ($p < 0.01$, max-fold change > 2, m/z range: 295–400) and showed the highest abundance in roots. These metabolite peaks were considered potential intermediates or side compounds of the triptolide biosynthetic pathway [31]. The Pearson correlation coefficient was calculated between each set of variables (either gene or metabolite) using MATLAB R2019b with a p-value < 0.05. Finally, the regulation networks of metabolites and TwWRKY genes were analyzed by Cytoscape software [61].

Subcellular localization

The ORF (open reading frame) of *TW23G00056.1* was amplified by polymerase chain reaction (PCR) using the Phusion high-fidelity PCR master mix (New England BioLabs, MA, USA) with specific primers from cDNA of *T. wilfordii*. Thereafter, the PCR product was ligated into the pEASY-Blunt Zero vector (TransGen Biotechnology, Beijing, China) and sequenced. The correct gene sequence of TW23G00056.1 was fused to the N-terminus of the green fluorescent protein (GFP) and ligated into the pAN580 vector. The pAN580-GFP was used as the control and the pAN580-NLS-mkate was selected as a marker for nuclear localization. Both pAN580-GFP/pAN580-NLS-mkate and pAN580-TW23G00056.1-GFP/pAN580-NLS-mkate were transformed into Arabidopsis protoplasts and the fluorescence was observed after incubation in darkness at 24 °C for 18–24 h.

Abbreviations

BLAST	Basic Local Alignment Search Tool
GFP	Green fluorescent protein
NCBI	National Center for Biotechnology Information
MeJA	Methyl jasmonate
ML	Maximum likelihood
Mw	Molecular weight
PCR	Polymerase chain reaction
PI	Isoelectric point
WGD	Whole genome duplication

Supplementary Information

The online version contains supplementary material available at https://doi.org/10.1186/s12864-025-11535-8.

Supplementary Material 1

Acknowledgements

We thank Yuhe Tu (Datian Taoyuan State Forest Farm in Fujian Province, Datian, China) and Sanbo Liu (China Resources Sanjiu (Huangshi) Pharmaceutical Co., Ltd. in Hubei province, Huangshi, China) for providing plant material of *T. wilfordii*.

Author contributions

Lm.T. and Lc.T. wrote the manuscript. W.G. and Lc.T. conceived and designed the experiments. Lm.T., Xy.Q., Jy.C., Yj.Z., Jh.G., Ss.Z., and Lc.T. analyzed the data and performed the study. W.G., Ss.Z., and Lc.T. supervised the research and reviewed the manuscript. All authors have read and agreed to the published version of the manuscript.

Funding

This work was supported by Zhejiang Provincial Natural Science Foundation of China (LQ23H280002), the National Natural Science Foundation of China (82204559), and Key project at central government level: The ability establishment of sustainable use for valuable Chinese medicine resources (2060302).

Data availability

The transcriptome and genomic data during the current study are available in the NCBI repository. The accession number of *T. wilfordii* genome sequence is JAAARO000000000, and the accession numbers of *TwWRKY* genes are listed in Table S1.

Declarations

Ethics approval and consent to participate
Not applicable.

Consent for publication
Not applicable.

Competing interests
The authors declare no competing interests.

Received: 2 December 2024 / Accepted: 27 March 2025
Published online: 24 April 2025

References

1. Ma B, Hu T, Li P, Yuan Q, Lin Z, Tu Y, Li J, Zhang X, Wu X, Wang X, et al. Phylogeographic and phylogenetic analysis for tripterygium species delimitation. Ecol Evol. 2017;7(20):8612–23.
2. Gao W, Liu MT, Cheng QQ, Pan GF, Wang XJ. Herbal textual research on tripterygium wilfordii. WORLD Chin Med. 2012;7(6):560–2.
3. Corson TW, Crews CM. Molecular Understanding and modern application of traditional medicines: triumphs and trials. Cell. 2007;130(5):769–74.
4. Kupchan SM, Court WA, Dailey RG Jr., Gilmore CJ, Bryan RF. Triptolide and Tripdiolide, novel antileukemic diterpenoid triepoxides from *Tripterygium wilfordii*. J Am Chem Soc. 1972;94(20):7194–5.
5. Zhou ZL, Yang YX, Ding J, Li YC, Miao ZH. Triptolide: structural modifications, structure-activity relationships, bioactivities, clinical development and mechanisms. Nat Prod Rep. 2012;29(4):457–75.
6. Graziose R, Lila MA, Raskin I. Merging traditional Chinese medicine with modern drug discovery technologies to find novel drugs and functional foods. Curr Drug Discov Technol. 2010;7(1):2–12.
7. Qiu D, Kao PN. Immunosuppressive and anti-inflammatory mechanisms of triptolide, the principal active diterpenoid from the Chinese medicinal herb *Tripterygium wilfordii* Hook. F. Drugs R D. 2003;4(1):1–18.
8. Zhang BJ, Wu YZ, Hao JL. The Pharmacological mechanism of triptolide and its research prospects in ophthalmology. Chin J Gerontol. 2009;29(24):3306–8.
9. Leuenroth SJ, Bencivenga N, Chahboune H, Hyder F, Crews CM. Triptolide reduces cyst formation in a neonatal to adult transition Pkd1 model of ADPKD. Nephrol Dial Transpl. 2010;25(7):2187–94.
10. Lue Y, Sinha Hikim AP, Wang C, Leung A, Baravarian S, Reutrakul V, Sangsawan R, Chaichana S, Swerdloff RS. Triptolide: a potential male contraceptive. J Androl. 1998;19(4):479–86.
11. Hikim AP, Lue YH, Wang C, Reutrakul V, Sangsuwan R, Swerdloff RS. Posttesticular antifertility action of triptolide in the male rat: evidence for severe impairment of cauda epididymal sperm ultrastructure. J Androl. 2000;21(3):431–7.
12. Liu Q. Triptolide and its expanding multiple Pharmacological functions. Int Immunopharmacol. 2011;11(3):377–83.
13. Chen BJ. Triptolide, a novel immunosuppressive and anti-inflammatory agent purified from a Chinese herb *Tripterygium wilfordii* Hook F. Leuk Lymphoma. 2001;42(3):253–65.
14. Kang DW, Lee JY, Oh DH, Park SY, Woo TM, Kim MK, Park MH, Jang YH. Min do S: Triptolide-induced suppression of phospholipase D expression inhibits proliferation of MDA-MB-231 breast cancer cells. Exp Mol Med. 2009;41(9):678–85.
15. Mujumdar N, Mackenzie TN, Dudeja V, Chugh R, Antonoff MB, Borja-Cacho D, Sangwan V, Dawra R, Vickers SM, Saluja AK. Triptolide induces cell death in pancreatic cancer cells by apoptotic and autophagic pathways. Gastroenterology. 2010;139(2):598–608.
16. Li CJ, Chu CY, Huang LH, Wang MH, Sheu LF, Yeh JI, Hsu HY. Synergistic anticancer activity of triptolide combined with cisplatin enhances apoptosis in gastric cancer in vitro and in vivo. Cancer Lett. 2012;319(2):203–13.
17. Liang M, Fu J. Triptolide inhibits interferon-gamma-induced programmed death-1-ligand 1 surface expression in breast cancer cells. Cancer Lett. 2008;270(2):337–41.
18. Brinker AM, Raskin I. Determination of triptolide in root extracts of *Tripterygium wilfordii* by solid-phase extraction and reverse-phase high-performance liquid chromatography. J Chromatogr A. 2005;1070(1–2):65–70.
19. Eulgem T, Rushton PJ, Robatzek S, Somssich IE. The WRKY superfamily of plant transcription factors. Trends Plant Sci. 2000;5(5):199–206.
20. Pandey SP, Roccaro M, Schon M, Logemann E, Somssich IE. Transcriptional reprogramming regulated by WRKY18 and WRKY40 facilitates powdery mildew infection of Arabidopsis. Plant J. 2010;64(6):912–23.
21. Liu J, Chen X, Liang X, Zhou X, Yang F, Liu J, He SY, Guo Z. Alternative splicing of rice WRKY62 and WRKY76 transcription factor genes in pathogen defense. Plant Physiol. 2016;171(2):1427–42.
22. Cao W, Wang Y, Shi M, Hao X, Zhao W, Wang Y, Ren J, Kai G. Transcription factor SmWRKY1 positively promotes the biosynthesis of Tanshinones in *Salvia miltiorrhiza*. Front Plant Sci. 2018;9:554.
23. Suttipanta N, Pattanaik S, Kulshrestha M, Patra B, Singh SK, Yuan L. The transcription factor CrWRKY1 positively regulates the terpenoid Indole alkaloid biosynthesis in *Catharanthus roseus*. Plant Physiol. 2011;157(4):2081–93.
24. Fu J, Liu Q, Wang C, Liang J, Liu L, Wang Q. ZmWRKY79 positively regulates maize phytoalexin biosynthetic gene expression and is involved in stress response. J Exp Bot. 2018;69(3):497–510.
25. Schluttenhofer C, Yuan L. Regulation of specialized metabolism by WRKY transcription factors. Plant Physiol. 2015;167(2):295–306.
26. Zheng Y, Jiao C, Sun H, Rosli HG, Pombo MA, Zhang P, Banf M, Dai X, Martin GB, Giovannoni JJ, et al. iTAK: A program for Genome-wide prediction and classification of plant transcription factors, transcriptional regulators, and protein kinases. Mol Plant. 2016;9(12):1667–70.
27. Song H, Sun W, Yang G, Sun J. WRKY transcription factors in legumes. BMC Plant Biol. 2018;18(1):243.
28. Yu H, Guo W, Yang D, Hou Z, Liang Z. Transcriptional profiles of SmWRKY family genes and their putative roles in the biosynthesis of Tanshinone and phenolic acids in *Salvia miltiorrhiza*. Int J Mol Sci. 2018;19(6):1593.
29. Liu SY, Xu Q, Chen NS. Expansion of photoreception-related gene families May drive ecological adaptation of the dominant diatom species. Sci Total Environ. 2023;897:165384.
30. Lu HZ, Li FR, Yuan L, Domenzain I, Yu R, Wang H, Li G, Chen Y, Ji BY, Kerkhoven EJ et al. Yeast metabolic innovations emerged via expanded metabolic network and gene positive selection. Mol Syst Biol. 2021;17(10):e10427.
31. Tu L, Su P, Zhang Z, Gao L, Wang J, Hu T, Zhou J, Zhang Y, Zhao Y, Liu Y, et al. Genome of *Tripterygium wilfordii* and identification of cytochrome P450 involved in triptolide biosynthesis. Nat Commun. 2020;11(1):971.
32. Zhou J, Hu T, Gao L, Su P, Zhang Y, Zhao Y, Chen S, Tu L, Song Y, Wang X, et al. Friedelane-type triterpene cyclase in Celastrol biosynthesis from *Tripterygium wilfordii* and its application for triterpenes biosynthesis in yeast. New Phytol. 2019;223(2):722–35.
33. Cui G, Duan L, Jin B, Qian J, Xue Z, Shen G, Snyder JH, Song J, Chen S, Huang L, et al. Functional divergence of diterpene syntheses in the medicinal plant *Salvia miltiorrhiza*. Plant Physiol. 2015;169(3):1607–18.
34. Shang Y, Ma Y, Zhou Y, Zhang H, Duan L, Chen H, Zeng J, Zhou Q, Wang S, Gu W, et al. Plant science. Biosynthesis, regulation, and domestication of bitterness in cucumber. Science. 2014;346(6213):1084–8.
35. Guo L, Winzer T, Yang X, Li Y, Ning Z, He Z, Teodor R, Lu Y, Bowser TA, Graham IA, et al. The *opium poppy* genome and morphinan production. Science. 2018;362(6412):343–7.
36. Su P, Guan H, Zhao Y, Tong Y, Xu M, Zhang Y, Hu T, Yang J, Cheng Q, Gao L, et al. Identification and functional characterization of diterpene synthases for triptolide biosynthesis from *Tripterygium wilfordii*. Plant J. 2018;93(1):50–65.
37. Yan H, Li M, Xiong Y, Wu J, da Silva JAT, Ma G. Genome-Wide characterization, expression profile analysis of WRKY family genes in *Santalum album* and functional identification of their role in abiotic stress. Int J Mol Sci. 2019;20(22):5676.
38. Ji N, Li Y, Wang J, Zuo X, Li M, Jin P, Zheng Y. Interaction of PpWRKY46 and PpWRKY53 regulates energy metabolism in MeJA primed disease resistance of Peach fruit. Plant Physiol Biochem. 2022;171:157–68.
39. Lian CL, Zhang F, Yang H, Zhang XY, Lan JX, Zhang B, Liu XY, Yang JF, Chen SQ. Multi-omics analysis of small RNA, transcriptome, and degradome to identify putative MiRNAs linked to MeJA regulated and Oridonin biosynthesis in Isodon rubescens. Int J Biol Macromol. 2024;258(Pt 2):129123.
40. Chugh R, Sangwan V, Patil SP, Dudeja V, Dawra RK, Banerjee S, Schumacher RJ, Blazar BR, Georg GI, Vickers SM, et al. A preclinical evaluation of Minnelide as a therapeutic agent against pancreatic cancer. Sci Transl Med. 2012;4(156):156ra139.
41. Zhou QY, Tian AG, Zou HF, Xie ZM, Lei G, Huang J, Wang CM, Wang HW, Zhang JS, Chen SY. Soybean WRKY-type transcription factor genes, GmWRKY13, GmWRKY21, and GmWRKY54, confer differential tolerance to abiotic stresses in Transgenic Arabidopsis plants. Plant Biotechnol J. 2008;6(5):486–503.
42. Alfieri M, Vaccaro MC, Cappetta E, Ambrosone A, De Tommasi N, Leone A. Coactivation of MEP-biosynthetic genes and accumulation of abietane

diterpenes in *Salvia sclarea* by heterologous expression of WRKY and MYC2 transcription factors. Sci Rep. 2018;8(1):11009.
43. Gao J, Zhang Y, Liu X, Wu X, Huang L, Gao W. Triptolide: Pharmacological spectrum, biosynthesis, chemical synthesis and derivatives. Theranostics. 2021;11(15):7199–221.
44. Zhang Y, Zhao Y, Wang J, Hu T, Tong Y, Zhou J, Gao J, Huang L, Gao W. The expression of TwDXS in the MEP pathway specifically affects the accumulation of triptolide. Physiol Plant. 2020;169(1):40–8.
45. Song Y, Chen S, Wang X, Zhang R, Tu L, Hu T, Liu X, Zhang Y, Huang L, Gao W. A novel strategy to enhance terpenoids production using cambial meristematic cells of *Tripterygium wilfordii* Hook. F. Plant Methods. 2019;15:129.
46. Su P, Gao L, Tong Y, Guan H, Liu S, Zhang Y, Zhao Y, Wang J, Hu T, Tu L, et al. Analysis of the role of geranylgeranyl diphosphate synthase 8 from *Tripterygium wilfordii* in diterpenoids biosynthesis. Plant Sci. 2019;285:184–92.
47. Tu L, Cai X, Zhang Y, Tong Y, Wang J, Su P, Lu Y, Hu T, Luo Y, Wu X, et al. Mechanistic analysis for the origin of diverse diterpenes in *Tripterygium wilfordii*. Acta Pharm Sinica B. 2022;12(6):2923–33.
48. Chen R, Bu Y, Ren J, Pelot KA, Hu X, Diao Y, Chen W, Zerbe P, Zhang L. Discovery and modulation of diterpenoid metabolism improves glandular trichome formation, Artemisinin production and stress resilience in *Artemisia annua*. New Phytol. 2021;230(6):2387–403.
49. Zerbe P, Chiang A, Dullat H, O'Neil-Johnson M, Starks C, Hamberger B, Bohlmann J. Diterpene synthases of the biosynthetic system of medicinally active diterpenoids in *Marrubium vulgare*. Plant J. 2014;79(6):914–27.
50. Zhang Y, Gao J, Ma L, Tu L, Hu T, Wu X, Su P, Zhao Y, Liu Y, Li D, et al. Tandemly duplicated CYP82Ds catalyze 14-hydroxylation in triptolide biosynthesis and precursor production in *Saccharomyces cerevisiae*. Nat Commun. 2023;14(1):875.
51. Zhang M, Zhao R, Huang K, Huang S, Wang H, Wei Z, Li Z, Bian M, Jiang W, Wu T, et al. The OsWRKY63-OsWRKY76-OsDREB1B module regulates chilling tolerance in rice. Plant J. 2022;112(2):383–98.
52. Wu Z, Li T, Cao X, Zhang D, Teng N. Lily WRKY factor LlWRKY22 promotes thermotolerance through autoactivation and activation of LlDREB2B. Hortic Res. 2022;9:uhac186.
53. Gu L, Hou Y, Sun Y, Chen X, Wang G, Wang H, Zhu B, Du X. The maize WRKY transcription factor ZmWRKY64 confers cadmium tolerance in Arabidopsis and maize (*Zea Mays* L). Plant Cell Rep. 2024;43(2):44.
54. Luo Y, Huang XX, Song XF, Wen BB, Xie NC, Wang KB, Huang JA, Liu ZH. Identification of a WRKY transcriptional activator from *Camellia sinensis* that regulates methylated EGCG biosynthesis. Hortic Res. 2022;9:uhac024.
55. Hansen NL, Kjaerulff L, Heck QK, Forman V, Staerk D, Møller BL, Andersen-Ranberg J. *Tripterygium wilfordii* cytochrome P450s catalyze the Methyl shift and epoxidations in the biosynthesis of triptonide. Nat Commun. 2022;13(1):5011.
56. Chen C, Chen H, Zhang Y, Thomas HR, Frank MH, He Y, Xia R. TBtools: an integrative toolkit developed for interactive analyses of big biological data. Mol Plant. 2020;13(8):1194–202.
57. Trapnell C, Pachter L, Salzberg SL. TopHat: discovering splice junctions with RNA-Seq. Bioinformatics. 2009;25(9):1105–11.
58. Anders S, Pyl PT, Huber W. HTSeq–a python framework to work with high-throughput sequencing data. Bioinformatics. 2015;31(2):166–9.
59. Anders S, Huber W. Differential expression analysis for sequence count data. Genome Biol. 2010;11(10):R106.
60. Rischer H, Oresic M, Seppanen-Laakso T, Katajamaa M, Lammertyn F, Ardiles-Diaz W, Van Montagu MC, Inze D, Oksman-Caldentey KM, Goossens A. Gene-to-metabolite networks for terpenoid Indole alkaloid biosynthesis in *Catharanthus roseus* cells. Proc Natl Acad Sci U S A. 2006;103(14):5614–9.
61. Shannon P, Markiel A, Ozier O, Baliga NS, Wang JT, Ramage D, Amin N, Schwikowski B, Ideker T. Cytoscape: A software environment for integrated models of biomolecular interaction networks. Genome Res. 2003;13(11):2498–504.

Publisher's note